Proceedings of IMECE2008
2008 ASME International Mechanical Engineering Congress and Exposition
October 31-November 6, 2008, Boston, Massachusetts, USA

IMECE2008-67924

BIOMECHANICAL DEVICE TOWARDS QUANTITATIVE MASSAGE

Hansong Zeng, Yi Zhao
Department of Biomedical Engineering
Ohio State University
Columbus, Ohio, USA
zhao.178@osu.edu

Timothy Butterfield
Department of Rehabilitation Sciences
University of Kentucky
Lexington, Kentucky, USA

Sudha Agarwal
Section of Oral Biology, School of Dentistry
Ohio State University
Columbus, Ohio, USA

Haq Furqan, Thomas Best
Department of Family Medicine
Ohio State University
Columbus, Ohio, USA

ABSTRACT

Massage therapies are widely employed for improving and recovering tissue functions and physical activities. It is generally believed that such therapies would promote health and well-being by many possible mechanisms, including fastening muscle blood flow, parasympathetic activity, releasing relaxation hormones and inhibiting muscle tension, neuromuscular excitability and stress hormones. Nonetheless, most of current research is based on statistics and thus qualitative, preventing the in-depth study of the effectiveness. This is partially due to the lack of appropriate tools for quantitative loading and in situ assessment of tissue performance.

To address this, we develop a biomechanical device to mimic massage therapies by applying controllable mechanical forces to animal tissues during cyclic mechanical motions. The device can apply compressive loads normal to the tissue surface and generate lengthwise motion along the tissue surface. Mechanical forces are applied with controllable magnitudes, frequencies and durations. Tissue mechanical response is recorded and correlated to the loading parameters. The changes of bulk tissue compliance and viscoelastic properties under various loading conditions are evaluated. The improvement of tissue functions and inhibition of muscle inflammation are examined. The results show that the peak torque production increased after massage, which suggests the recovery of muscle functions. A reduced number of infiltrating leukocytes is also observed in the subject muscle fibers after massage. Findings of this study suggest that the biomechanical device offers a quantitative analysis of massage actions, which will help to determine the optimal range of loading conditions required for safe and effective use of massage therapies.

INTRODUCTION

Massage therapies have been used for thousands of years to improve human health and well-being. In fact, such therapies make up approximately 45% of the total physiotherapy treatments provided for muscle ailments [1]. It is a general belief that massage reduces muscle tension, excitability, and stress hormones, as well as increases the blood flow and parasympathetic activities [2-6]. Clinical research has provided modest evidence that massage therapies are effective in promoting muscle recovery from injury [6-9], alleviating lymphedema [10-12], and relieving lower back pain [13-15].

Massage elicits a biological response which is a synergistic combination of several complex processes controlled by interrelated factors, such as viscoelastic deformation of the tissue, biomechanical transduction and signaling, and psychophysiologic reactions. These observations have been confirmed by many studies aimed at exploring mechanisms responsible for the effectiveness of massage [16-20]. Swedish and Thai massages have been shown to improve physiological and psychological symptoms as assessed by blood pressure, heart rate, and range of limb motion, as well as anxiety and mood [21]. Similarly, massage-like stroking was shown to decrease plasma levels of gastrin, insulin and somatostatin, as well as increase blood glucose levels [22], and facilitate recovery of neuromuscular function [23].

Due to the effectiveness of massage, there has been a concomitant increase in the development of robotic massage systems and investigations to explain the mechanisms of massage actions beyond qualitative observations and anecdotal experiences. In an effort to accurately deliver mechanical forces and to mimic manual massage, several systems have been developed. For example, Jones et al. have used a robotic system to apply controlled forces, where robot fingers move along a pre-designed trajectory [24]. Similarly, Minyong et al. designed

a controlled multi-fingered robot to simulate the hand of a manual therapist [25]. Most of current robotic systems apply mechanical loads on tissue by indentation at a controlled force (Figure 1a), similar to the tapping techniques and Shiatsu massage. These efforts have provided a good starting point and a promising solution for performing controlled massage on target tissues. It is also possible that such robotic system might be an improvement over human manual therapies that are often plagued by uncontrolled and varying loading conditions.

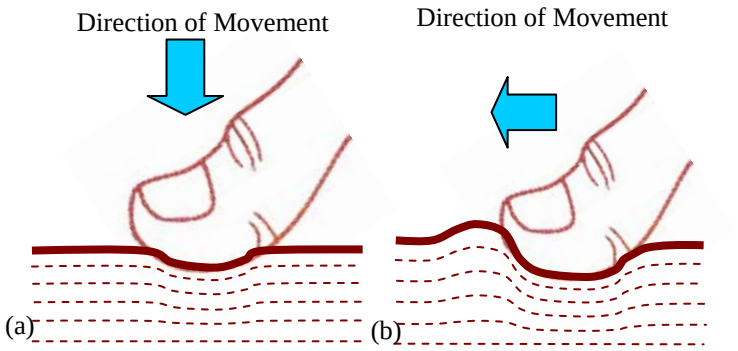

Fig. 1: *Two type of massage techniques. (a) The compressive loading is applied to the tissue by repetitive up and down movement at the same site on the surface of subject tissue; (b) In the lengthwise motion, the massage head (or thumb) moves in the direction parallel to the natural surface of the tissue. The dashed lines illustrate the deformation of the tissues underneath the surface.*

Massage practitioners believe that lengthwise strokes parallel to the natural surface of the tissue (Figure 1b) plays a significant role in relieving the patient's symptoms by unblocking tissue energy blockages and reintroducing optimal flow of energy [26]. Studies have shown that such motion during massage is effective in dilating the blood vessels of skeletal muscle and improving blood flow in the tissue [27, 28]. Therefore, it is important to understand the significance of lengthwise strokes on the efficacy of massage in order to harness its most beneficial effects.

In this study, we designed, fabricated and tested a biomechanical device which applies compressive loads and lengthwise strokes simultaneously to rabbit skeletal muscle. The massage head of the device applies compressive loads while traveling in parallel to the tissue surface. This type of mechanical loading is common to the effleurage and rubbing techniques of Swedish or similar types of massage actions. The loading doses can be determined with the help of motion analysis. Changes of viscoelastic properties and tissue function in response to mechanical loading during the lengthwise massage strokes demonstrate the effectiveness of the device for mimicking manual massage. This device is expected to elucidate tissue biomechanical behavior under massage and the molecular basis of beneficial effects in massage actions.

ANIMAL PREPARATION

All animal experiments were performed following approval by the Institutional Laboratory of Animal Care & Use Committee at the Ohio State University. New Zealand white rabbits (16-18 weeks old) were sedated with 0.25 ml acepromazine. Subsequently, animals were anesthetized with a mixture of oxygen and vaporized isoflurane and were kept under anesthesia throughout the course of the experiment. Once anesthetized, the rabbit hind limb was placed on a flat surface in parallel to the traveling path of the kneading wheel described below.

MASSAGE DEVICE

The key components of the biomechanical device for quantitative massage include a computer-controlled linear motion system for applying compressive loading and a pneumatic actuator for generating lengthwise strokes. Prior to application of mechanical loading, the anesthetized rabbit was placed on the stage to expose the tissue of interest (lower leg) to the PVC kneading wheel. The leg was firmly fixed on the stage to limit mechanical vibrations and extremity movement. The kneading wheel was gently lowered to apply compressive loads to the leg. Loading magnitude was controlled by changing the latitude of the kneading wheel. The frequency of the lengthwise strokes was controlled with a linear pneumatic actuator, mimicking the effleurage strokes of the finger tips or the palm of human hands. Repetitive cycling of the pneumatic actuator was controlled using a three-way solenoid valve, which was regulated by a digital function generator through an electric relay. The function generator was used to adjust the frequency of mechanical loads. Travel velocity of the kneading wheel was monitored by a compressive air pump through a pneumatic regulator. Mechanical forces applied to the rabbit's lower leg were recorded using a force sensor (PASCO INC., US), and transferred to a PC through a NI 6221 data acquisition system for subsequent analysis. Movement of the kneading wheel was monitored using a digital video camera. Velocity and acceleration were derived from motion analysis of the captured video frames. Before and after each experiment, the tissue compliance and viscoelastic properties were determined by the device.

ASSESSMENT OF TISSUE MECHANICAL PROPERTIES

Tissue Compliance

Compliance is a frequently used parameter in tissue biomechanics to describe the mechanical properties of biological tissues [29]. It is defined as the inverse of stiffness [30] and can be experimentally determined by applying a compressive force F normal to the tissue:

$$Compliance = \frac{\Delta}{F} \quad (1)$$

where Δ is the deformation of the tissue along the direction of the applied force [31, 32]. According to prior research and massage therapists [6, 33], the compliance of tissue is inversely related to the level of tissue tension, i.e., highly tensioned tissues have low compliance. This, along with the psychophysiological conditions of the patient/tissue, provides useful guidance for therapists to make their decision of appropriate massage protocols. In addition, the compliance of tissue also depends upon mechanical loadings. For example, the compliance of an athlete's muscles tends to increase after a

Swedish massage [34]. Therefore, the quantitative determination of tissue compliance is important for the design, optimization and assessment of massage therapies.

The compliance of the tibialis anterior (TA) was measured by applying a compressive load to the rabbit's anterior lower limb. The loading head driven by the linear motor system was indented on the tissue at 1.27 mm/s. Contact force was measured at the sampling rate of 24 Hz. Resolution of the z-axis movement was 20 μm, and the resolution of compressive force was 0.2N. To reduce geometric influence, the surface under loading was essentially flat and normal to the z-axis. The force range for slope calculations was limited to 1–4 N. A maximum indentation force of 18 N was used to ensure that the pressure during the test would not injure the tissue. The range of the slope was limited to 1–2 N/s. The subject tissue was marked with an ink marker so that the same site was repeatedly tested. Each site was preconditioned with 3–5 compressions. The mean values of the force-displacement slope with the force ranging from 1–4 N were calculated. A representative loading curve is shown in Figure 2, where the compliance of the rabbit hind limb was calculated to be 1.33±0.22 mm/N.

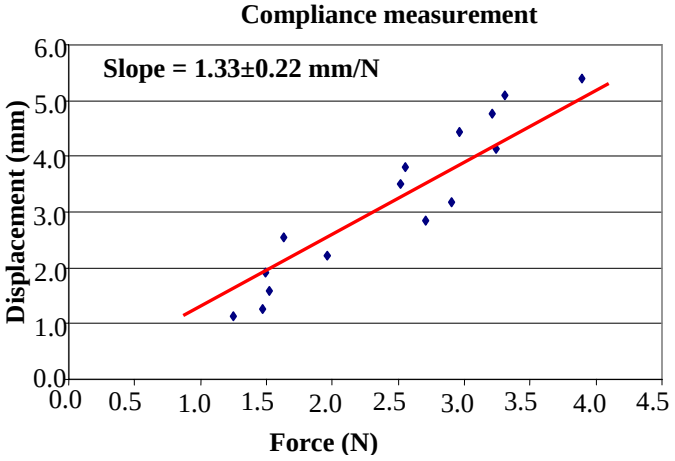

Fig. 2: *Tissue compliance measurement.*

Viscoelastic Behavior

Like most biologic tissues, the rabbit lower leg demonstrates non-linear viscoelastic behavior. Such behavior may vary under different physiological conditions. For example, when muscle tissues swell following trauma, e.g. compartment syndrome, the tissues may demonstrate a different viscoelastic behavior as the fluid accumulates within a confined space [35]. For our study, the viscoelastic properties of the tissue were evaluated using a ramp-and-hold relaxation test. Mechanical loading was applied to the tissue at a high loading rate (18 N mechanical force was loaded on the tissue in less than 0.1 second) to approximate the ideal 'sudden' stress. In this work, only one loading rate was used because the viscoelastic properties of the muscle and surrounding tissues are essentially rate-independent [36, 37]. During the holding, tissue deformation was kept constant and the compressive forces were continuously recorded. Figure 3 shows a representative relaxation process of the tissue before massage. Both fast and slow relaxations were determined from the measurement. The relaxations were exponential with time and can be characterized by the time taken for the tension to decay to half-value. In this case, the half-value time of the rapid relaxation was 2.74 s; and the half-value time of the slow relaxation was 65.38 s. Experiments showed that these values changed with mechanical loadings, which can likely be attributed to the changes of limb morphology, elastin and collagen mechanical properties, and the blood [38].

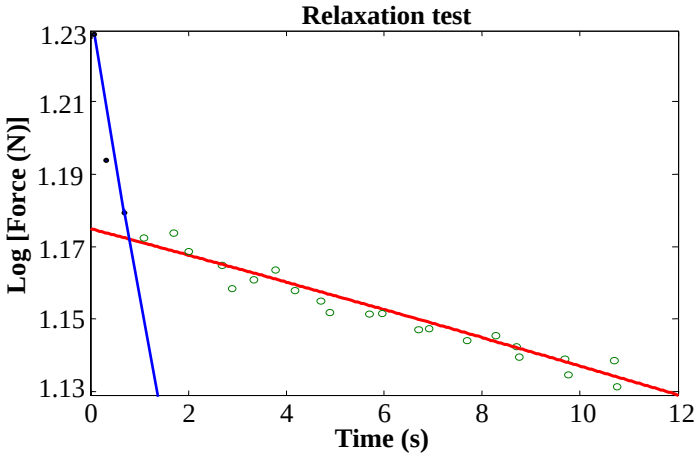

Fig. 3: *Relaxation test is performed on the rabbit hind limb, where the fast and slow relaxation time constants can be determined.*

MECHANICAL LOADING DURING LENGTHWISE STROKES

During the lengthwise strokes, the kneading wheel moved back and forth and applied compressive loads to the area of contact. Tissue at different positions was subject to different amounts of loads. The outcome may show a spatial variation because the tissue thickness, traveling velocity of the kneading wheel and the compressive loading all varied along the traveling direction.

Since there is not a generally accepted term to describe the "dose" during the lengthwise strokes of the kneading wheel, a parameter was needed to represent the loading status of the subject tissue. We examined a specimen of the tissue with an infinitely small length δ (Figure 4a). The width of this slice was *w*. The distance between the skin and the bone was *Th*. In order to simplify the analysis, we assumed the width (*w*) along x axis and the thickness (*Th*) along the y-axis were constant within the region of interest. Tissue loading was therefore analyzed using a 2D model (Figure 4b), where the kneading wheel traveled along the x-axis and the normal loading was applied to the rabbit tissues along the z-axis. Since the length (δ) is much smaller than the curvature radius of the loading wheel, it was assumed that the stress over the cross sectional area ($w \times \delta$) was homogeneous.

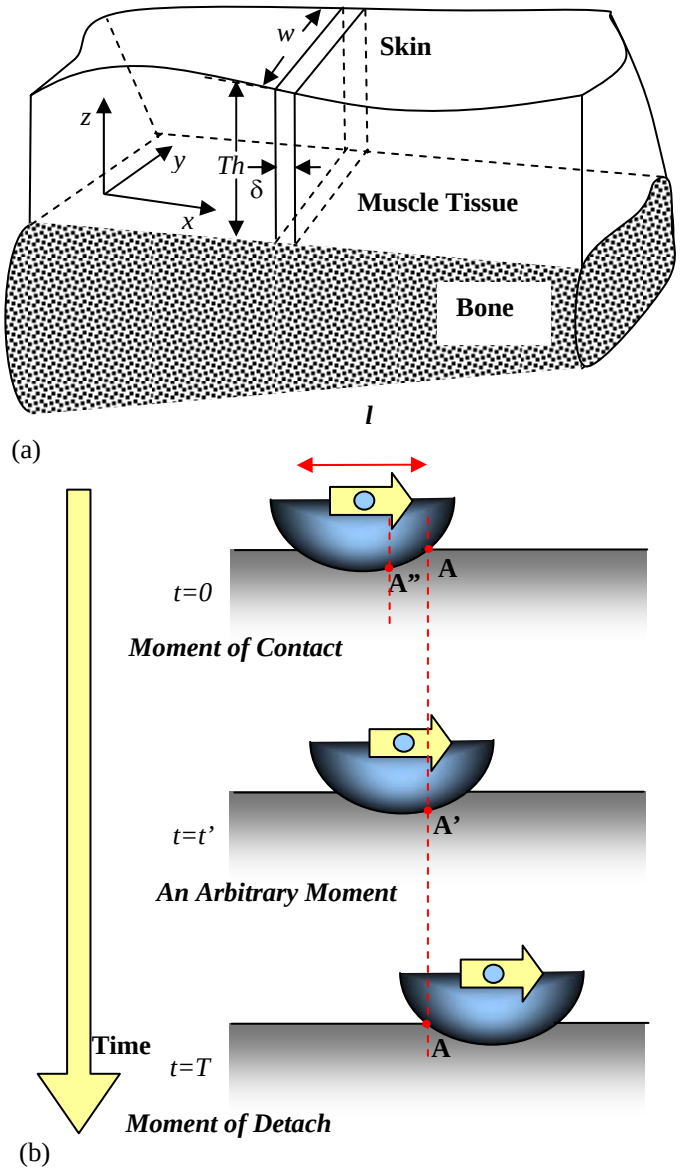

Fig. 4: *The mechanical loads applied on the tissue were analyzed using a simplified model. (a) a small specimen of rabbit tissue with dimensions (δ×w×Th). (b) The time domain was connected with the spatial domain by assuming the forces applied to the corresponding points (A' and A") are the same.*

During each cycle, the mechanical force started to load on the point of interest A once the kneading wheel contacted with the point, and ended as they separated. At any arbitrary moment ($t=t'$) during the cycle, point A deformed to point A'. The loading dose was expressed by integrating the mechanical force over the contact time as $\int_0^T F(t)dt$, where T is the entire contact time during each contact, and $F(t)$ is the contact force within the area ($w\times\delta$) at time t. Given the small contact length (l) and the large traveling velocity of the kneading wheel, we approximated that the wheel traveled at a constant velocity when passing the point A. Furthermore, since the contact length (l) was much smaller than the characteristic radius of curvature of the subject tissue, it was assumed that at any arbitrary moment $t=t'$ during the contact, the contact forces at the following two points were the same: (i) point A' under compressive loading at the time t', and (ii) point A" under compressive loading at the time 0 (start of contact), where A' and A" were at the same depths. Therefore, the loading dose can be rewritten using parameters in the spatial domain, as:

$$\int_0^T F(t)dt = \frac{1}{v(x)}\int_0^l F(x)dx = \frac{F_{meas}\delta}{v(x)} \quad (2)$$

The loading dose per unit volume can be obtained by dividing the loading dose by the volume ($w\times\delta\times Th$) as:

$$Dose(x) = \frac{F_{meas}(x)}{w\times v(x)\times Th(x)} \quad (3)$$

From this equation, the loading dose which was applied to a defined point on the subject tissue during a single loading process was estimated. Furthermore, the total loading dose of cyclic motion was obtained by:

$$Dose(x) = \frac{F_{meas}(x)\times 2N}{w\times v(x)\times Th(x)} \quad (4)$$

where N is the number of cycles of the operation. The factor 2 is used since the tissue is subject twice to the loading force during each cycle.

Eqs. (3, 4) show that the loading dose during the lengthwise strokes can be estimated using a simple form. The dose is a function of the width and thickness of the subject tissue, the applied force and the traveling velocity of the lengthwise strokes. Thus for a defined tissue, the dose can be adjusted by changing the magnitudes of the applied forces, the velocity of the kneading wheel and the number of loading cycles. It was also noted from Eqs. (3, 4) that the loading dose is independent of the geometries of the kneading wheel.

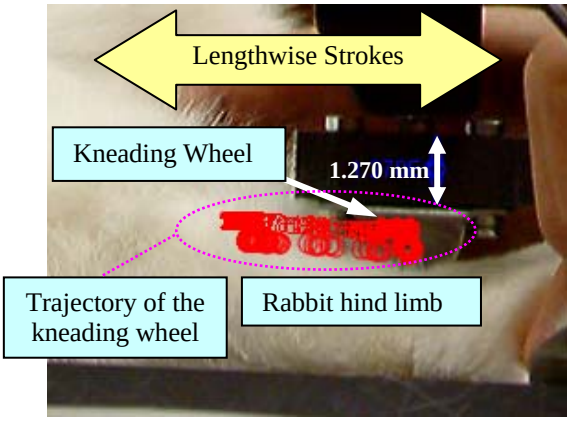

Fig. 5: *Real time analysis of the lengthwise motion of the kneading wheel on the rabbit lower limb.*

To experimentally determine the loading dose, the transverse motion of the kneading wheel was analyzed from the video frames captured by a digital video camera. In particular, the position of the kneading wheel was obtained by tracking a characteristic point**.** The velocity was calculated from the first order derivative of the position (Figure 5). The curve of compressive loading force *versus* position was thus derived.

According to Eq. (4), the loading dose is also a function of the tissue thickness (the distance from the skin to the bone). A piece of thick tissue is subject to a lower dose than a piece of thin tissue under the same loading conditions. Due to technical

complexity of non-invasive measurement of tissue thickness, we assume two thickness profiles for the determination of the loading dose based on the shape of the rabbit hind limb: (a) a constant thickness of ~ 7.5 mm and (b) an exponentially varying thickness from ~5.0 mm to ~ 10.0 mm over the entire length of the hind limb of ~25.0 mm. The results showed that assuming a constant thickness leads to large dose variation while an exponentially varying thickness leads to small loading dose variation along the x-axis, especially in the middle part of the hind limb. Research is underway to experimentally determine tissue thickness along the lengthwise direction.

MECHANICAL PROPERTIES BEFORE AND AFTER LENGTHWISE STROKES

The evolution of the tissue compliance and viscoelastic properties was measured at a defined position in the middle part of the rabbit hind limb. These properties were obtained before loading and immediately after each experiment. It is seen from Figure 6 that the compliance increased with loading dose of the lengthwise strokes (i.e., the tissue became softer). Tissue compliance increased ~ 36.3% in the first 100 cycles (loading dose: $8.4\times10^{7}\,N\cdot s/m^{3}$). During the following 200 cycles (loading dose: $2.52\times10^{8}\,N\cdot s/m^{3}$), compliance changed less than half as fast and increased ~ 47.6% as compared to the original value. Finally, tissue compliance after 900 cycles (loading dose: $7.55\times10^{8}\,N\cdot s/m^{3}$) was ~ 61.2% more than the original value. This suggests that the initial loading of lengthwise strokes is most effective in increasing the tissue compliance, while the following loading has limited effect.

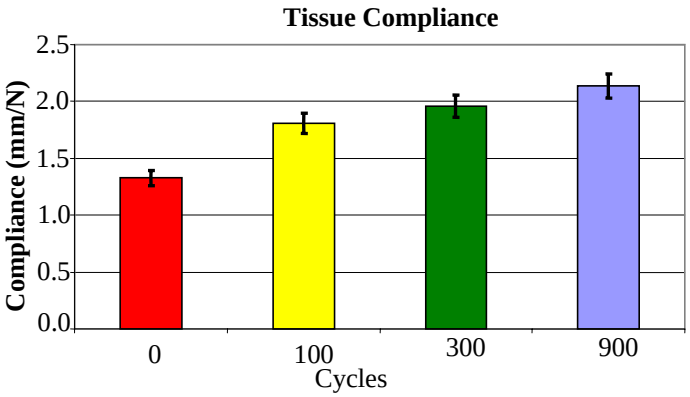

Fig. 6: *Tissue compliance increased ~ 36.3% after 100 cycles, ~ 47.6% after 300 cycles and ~ 61.2% after 900 cycles. The error bars indicate variation in the measurements.*

The viscoelastic properties were also a function of the lengthwise strokes. Figure 7 show the changes of the half-value time of the fast and slow relaxation. In both case, it is clear that the half-value time has the tendency to decrease after mechanical loading, which suggests that the tissue became "*more viscous*" upon the lengthwise strokes. However, the change of the half-value time is not monotonic quantity. This may due to the dynamic tissue response to the lengthwise strokes. More extensive investigation is needed to address such viscoelastic behavior.

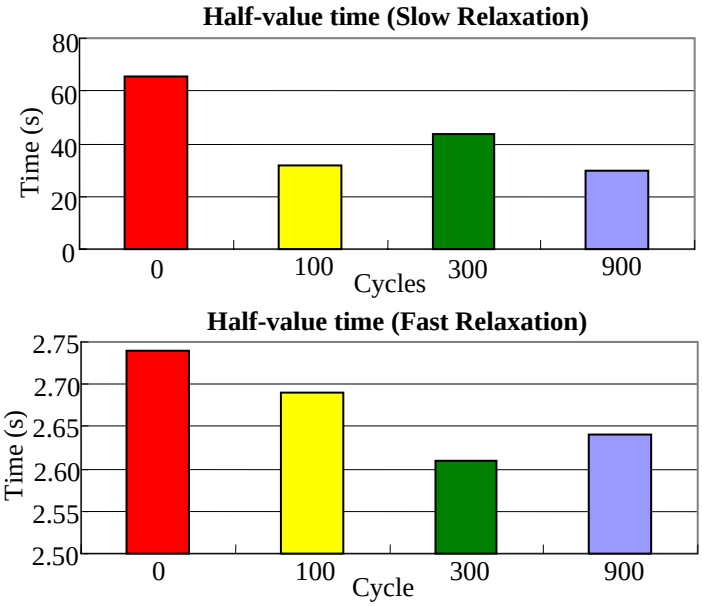

Fig. 7: *Relaxation test showed the hind limb became "more viscous" after lengthwise strokes, as evidenced by the changes of the half-value time in slow and fast relaxation. For slow relaxation, the half-value time quickly dropped from 65.38 s (before loading) to 31.8 s after 100 cycles (reduced more than 51.4%); In fast relaxation, a relatively small change was observed (1.8%, from 2.74 s before loading to 2.69 s after 100 cycles). In the following cycles, half-value time did not change monotonically. After 300 cycles, the half-value times are 43.52 s for slow relaxation and 2.61 s for fast relaxation. After 900 cycles, the half-value times are 30.00 s for slow relaxation and 2.64 s for fast relaxation.*

TISSUE FUNCTION IMPROVEMENT WITH MASSAGE

Functional improvement of the rabbit hind limbs under the lengthwise strokes was investigated by examining the recovery of muscle function following eccentric exercise-induced damage. After adequate anesthesia as described above, the rabbit was secured supine in a sling with one foot attached to a footplate, which was connected to a torque sensor on the cam of a servo-motor. Repetitive eccentric exercise was applied to the hind limb from a tibiotarsal angle of 95° to 145° of plantar flexion at angular velocity of 2.62, inducing ~ 70% loss of peak torque production.

Lengthwise massage strokes were applied at a frequency of 0.5 Hz for 900 cycles per day for four consecutive days. The average magnitude of the compressive force was about 11.4 N. Peak isometric torque following four days of lengthwise strokes of mechanical loading improved up to 117% following exercise, compared to only a 26% increase in the contralateral rested limb (Figure 8). Minimal muscle fiber damage and infiltrating leukocytes were observed (similar to that in the muscle before loading) in the muscles subject to lengthwise massage strokes (shown in the subfigures), while extensive infiltrating leukocytes and torn fibers were seen in the non-massaged muscle immediately following the eccentric exercise.

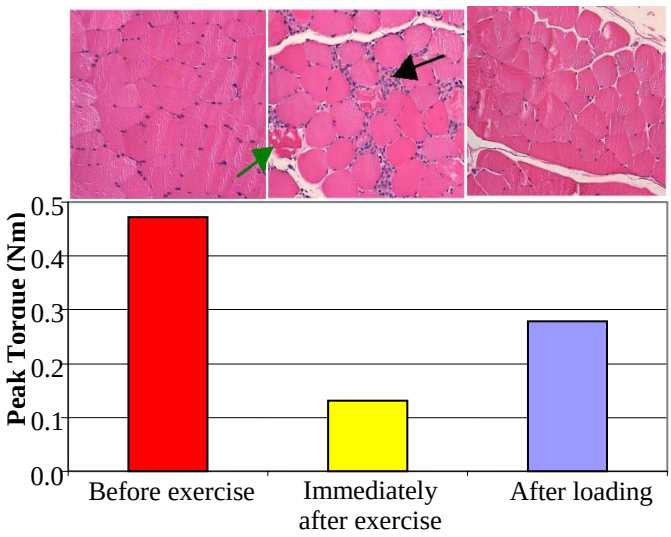

Fig. 8: *Lengthwise strokes showed striking effects on recovering the post-exercise muscle damage. After lengthwise massage of 30 minutes per day (0.5Hz) for 4 consecutive days (average load of about 11.4 N), the peak toque of the tissue increased 117% than that of the tissue immediately following the eccentric exercise. The minimal muscle fiber damage and infiltrating leukocytes were also observed (shown in the subfigures). The green arrow indicates the torn muscle fiber. The black arrow indicates the increased level of infiltrating leukocytes.*

CONCLUSION

A biomechanical device capable of applying precisely controlled lengthwise strokes in cyclic motion is developed to mimic rubbing and effleurage-like motions exerted during massage therapies, and to assess the effectiveness of massage actions. Results of this study demonstrate that the device can deliver simultaneous compression and lengthwise motion effectively as assessed by the regulation of the tissue compliance and the viscoelastic properties of the rabbit hind limb tissues. The functional improvement of damaged tissues is validated using an animal model with post-exercise injury. The device provides a promising starting point for quantitative application and assessment of massage therapy, which will shed light on the understanding of mechanism and the beneficial/adverse effects of mechanical signals in muscle tissues.

ACKNOWLEDGMENTS

This work was partially supported by Mathematical Bioscience Institute at the Ohio State University.

REFERENCES

[1] Galloway S, Watt J, and Sharp C, Massage provision by physiotherapists at major athletics events between 1987 and 1998. Br J Sports Med 2004, 38(2): 235-237.
[2] Mars M, Maharaj SS, and Tufts M, The effect of compressed air massage on skin blood flow and temperature. Cardiovascular Journal of South Africa, 2005, 16(4), 215-219.
[3] Mori H, Ohsawa H, Tanaka TH, Taniwaki E, Leisman G, and Nishijo K, Effect of massage on blood flow and muscle fatigue following isometric lumbar exercise. Medical Science Monitor, 2004, 10(5), CR173-178.
[4] Li X, Hirokawa M, Inoue Y, Sugano N, Qian S, and Iwai T, Effects of acupressure on lower limb blood flow for the treatment of peripheral arterial occlusive diseases. Surgery Today. 2007, 37(2), 103-108.
[5] Tochikubo O, Ri S, and Kura N, Effects of pulse-synchronized massage with air cuffs on peripheral blood flow and autonomic nervous system. Circulation Journal, 2006 70(9), 1159-1163.
[6] Weerapong P, Hume PA, and Kolt GS, The mechanisms of massage and effects on performance, muscle recovery and injury prevention. Sports Med, 2005, 35(3), 235-256.
[7] Hu J, Zhang XL and Yan JT, Effects of massage on satellite cells of acute contusive skeletal muscles. Journal of Acupuncture and Tuina Science, 2007, 5(1), 6-9.
[8] Tiidus PM, Manual massage and recovery of muscle function following exercise: a literature review. Journal of Orthopedic and Sports Physical Therapy, 1997, 25(2), 107-112.
[9] Tiidus PM, and Shoemaker JK, Effleurage massage, muscle blood flow and long-term post-exercise strength recovery. International Journal of Sports Medicine, 1995, 16(7), 478-483.
[10] Bernas M, Witte M, Kriederman B, Summers P, and Witte C, Massage therapy in the treatment of lymphedema. Engineering in Medicine and Biology Magzine, March/April 2005, 58-68.
[11] Warren AG, Brorson H, Borud LJ, and Slavin SA, Lymphedema: a comprehensive review. Annals of Plastic Surgery, 2007, 59(4), 464-72.
[12] Linnitt N, and Davies R, Fundamentals of compression in the management of lymphoedema. British Journal of Nursing, 2007, 16(10), 588, 590, 592.
[13] Ernst E, Massage therapy for low back pain: a systematic review. J Pain and Symptom Management, 1999, 17(1), 65-69.
[14] Zullino DF, Krenz S, Fresard E, Cancela E, and Khazaal Y, Local back massage with an automated massage chair: general muscle and psychophysiologic relaxing properties. Journal of Alternative and Complementary Medicine, 2005, 11(6), 1103-1106.
[15] Eguchi A, Effect of static stretch on fatigue of lumbar muscles induced by prolonged contraction. Electromyogr Clin Neurophysiol, 2004, 44(2), 75-81.
[16] Cowen VS, Burkett L, Bredimus J, Evans DR, Lamey S, Neuhauser T, and Shojaee L, A comparative study of Thai massage and Swedish massage relative to physiological and psychological measures. Journal of Bodywork and Movement Therapies, 2006, 10(4), 266-275.
[17] Hur MH, Oh H, Lee MS, Kim C, Choi AN, and Shin GR, Effects of aromatherapy massage on blood pressure and lipid profile in korean climacteric women. International Journal of Neuroscience, 2007 117(9), 1281-1287.
[18] Bost N, and Wallis M, The effectiveness of a 15 minute weekly massage in reducing physical and psychological stress in nurses, Australia Journal of Advanced Nursing. 2006, 23(4), 28-33.
[19] Fang CS, and Liu CF, Applying back massage protocol to promote an intensive care unit patient's quality of sleep. Hu Li Za Zhi, 2006, 53(6), 78-84.

[20] Field T, Diego M, and Hernandez-Reif M, Prematurity and potential predictors. International Journal of Neuroscience, 2008 118(2), 277-289.
[21] Anderson PG, and Cutshall SM, Massage therapy: a comfort intervention for cardiac surgery patients. Clinical Nurse Specalist, 2007, 21(3), 161-165.
[22] Holst S, Lund I, Petersson M, and Uvnas-Moberg K, Massage-like stroking influences plasma levels of gastrointestinal hormones, including insulin, and increases weight gain in male rats. Autonomic Neuroscience: Basic and Clinical, 2005, 120(1-2), 73-79.
[23] Solodkov1 AS and Povareshchenkova YA, Dynamics of neuromuscular system recovery as a consequence of various massage techniques as determined from electroneuromyography parameters. Human Physiology, 2006, 32(5), 110-120.
[24] Jones KC, and Du W, Development of a massage robot for medical therapy. Procedding of IEEE/ASME International Conference of Advanced Intelligent Mechatronics, 2003, 2, 1096-1101.
[25] Minyong P, Miyoshi T, Terashima K, and Kitagawa H, Expert massage motion control by multi-fingered robot hand. Proceedings of International Conference on Intelligent Robots and Systems, 2003, 3, 3035-3040.
[26] Hankey A, CAM and the phenomenology of pain, Evidence-based Complementary and Alternative Medicine, 2006, 3(1), 139-41.
[27] Fernandez-de-las-Penas C, Alonso-Blanco C, Fernandez-Carnero J, and Miangolarra-Page JC, The immediate effect of ischemic compression technique and transverse friction massage on tenderness of active and latent myofascial trigger points: a pilot study. J Bodywork Movement Therapies, 2006, l0(1), 3-9.
[28] Gregorya MA and Mars M, Compressed air massage causes capillary dilation in untraumatised skeletal muscle: a morphometric and ultrastructural study. Physiotherapy, 2005, 91(3), 131–137.
[29] Fung YC, Biomechanics: mechanical properties of living tissues (2nd ed.), Springer, New York, 1993.
[30] Silver-Thorn MB, In vivo indentation of lower extremity limb soft tissue. IEEE Transaction of Rehabilitation Engineering, 1999, 7(3), 268-277.
[31] Vannah WM and Childress DS, Indentor tests and finite element modeling of bulk muscular tissue in vivo, Journal of Rehabilitation Ressearch and Development, 1996, 33(3), 239-252.
[32] Pathak AP, Silver-Thorn MB, Thierfelder CA, and Prieto TE, A rate-controlled indentor for in vivo analysis of residual limb tissues, IEEE Transaction of Rehabilitation Engineering, 1998, 6(1), 12-20.
[33] Bank AJ, and Kaiser DR, Smooth muscle relaxation: effects on arterial compliance, distensibility, elastic modulus, and pulse wave velocity, Hypertension, 32(2), 1998, 356-359.
[34] Hemmings BJ, Physiological, psychological and performance effects of massage therapy in sport: a review of the literature. Physical Therapy in Sport, 2001, 2(4), 165-170.
[35] Ostrander LE, Cui W, Groskopf R, and Lee BY, Viscoelasticity of bulk limb tissue, Proceedings of the Annual International Conference of the IEEE Engineering in Engineering in Medicine and Biology Society, 1989, 5, 1421-1422.
[36] Holzapfel GA, Gasser TC and Stadler M, A structural model for the viscoelastic behavior of arterial walls: continuum formulation and finite element analysis, Europe ournal of Mechanics A - Solids, 2002, 21(3), 441-463.
[37] Weiss JA, Gardiner JC and Bonifasi-Lista C, Ligament material behavior is nonlinear, viscoelastic and rate-independent under shear loading, Journal of Biomechanics, 2002, 35(7), 943-950.
[38] Abbott BC, and Lowy J, Stress relaxation in muscle, Proceedings of the Royal Society of London. Series B, Biological Sciences, 1957, 146 (923), 281-288.